

Ultrasonic Thermoacoustic Energy Converter

 Myra Flitcroft & Orest G. Symko¹

University of Utah Department of Physics & Astronomy

Salt Lake City, UT 84112

orest@physics.utah.edu

Abstract

Thermoacoustic prime movers have been developed for operation in the low ultrasonic frequency range by scaling down the device size. The developed engines operate at frequencies up to 23 kHz. They are self-sustained oscillators whose dimensions scale inversely with operating frequency. The smallest one being 3.4mm long with a 1mm diameter bore, i.e. the engine inner volume of 2.67 mm³. The generated sound levels reached intensities in the range of 143 dB – 150 dB in the low ultrasonic range. The miniaturization of thermoacoustic engines will lead to the development of device arrays.

Keywords: ultrasonic, thermoacoustic, energy converter, heat engine

1. Introduction

Usually when a new device is developed it tends to be large and bulky, and eventually as its application demands become more diverse, the device is scaled down in size. Quite often it becomes the basic unit for array configuration. There are many examples of miniaturization which led to new applications. In this paper, the development and scaling down in size of thermoacoustic engines is presented. Reasons for miniaturizing such devices are based on certain advantages that such an approach would bring, and on specific applications in energy conversion. The development of thermoacoustic devices in recent years has escalated as a variety of applications has been identified. [1-4] In the work presented here the development is towards miniature thermoacoustic devices, working in the low ultrasonic frequency range and their application for energy conversion. More specifically one interesting application is the conversion of waste heat to electrical energy.

A thermoacoustic device, known as a prime mover, converts heat to sound in an acoustic resonator. Heat is injected to a heat exchanger, the hot heat exchanger, inside the resonator. This exchanger is in thermal contact with a stack or bundle of large surface area material (such as steel wool); at the other end of the stack, a cold heat exchanger is in thermal contact with it. This cold side is usually anchored thermally to ambient temperature. Such a device is a heat engine operating between a hot and cold heat sink and it is driven to oscillate by a temperature gradient along the stack [5]. The working fluid is gas, and in the work presented here it is air at atmospheric pressure. The acoustic oscillations are generated at a threshold temperature gradient and they are sustained by positive feedback and by heat input at the hot heat exchanger. [6, 7] This device belongs to the class of self-sustained oscillators, characterized by nonlinear dynamics [8]. Being a resonant system, the operating frequency varies inversely with the resonator dimensions [9]. In order to achieve energy conversion from heat to electricity a piezoelectric device is attached via an acoustic cavity to the resonator of this acoustic device.

The interaction of the sound field with the elements of the stack is thermal and viscous. It is characterized by a thermal penetration depth δ_κ and a viscous penetration depth δ_ν . They are given by

$$\delta_\kappa = (2\kappa / \omega)^{1/2} \quad (1)$$

$$\delta_\nu = (2\nu / \omega)^{1/2} \quad (2)$$

where ω is the angular frequency, κ the thermal diffusivity and ν the kinematic viscosity of the gas. Those distances are important for scaling the device for high frequency operation.

¹ Email address: orest@physics.utah.edu (Orest G. Symko)

The acoustic device is a heat engine, and its performance is characterized by its efficiency and power density. Compared to the efficiency of a Carnot engine, the thermoacoustic efficiency η is approximated by [6]

$$\eta = \frac{1}{\Gamma} (\Delta T / T_m) \quad (3)$$

where ΔT is the temperature difference along the stack, between the hot and cold heat exchangers, T_m is the mean temperature, and Γ is the ratio of temperature gradient ∇T along the stack normalized to a critical temperature gradient ∇T_{crit} which determines the onset for oscillations. For simplicity here, viscous losses are not included in this. The Carnot efficiency (for no load) is approximately $(\Delta T / T_m)$. For prime mover operation Γ should be greater than 1, i.e. the temperature gradient needs to be larger than the critical temperature gradient. This threshold gradient is determined by the exchange of heat between the stack and the sound field, following a displacement of the air parcels of the sound field relative to the stack temperature gradient. It is given by

$$\nabla T_{\text{crit}} = \frac{\gamma - 1}{T_m \beta} \frac{T_m}{\lambda} \tan\left(\frac{x}{\lambda}\right) \quad (4)$$

where γ is the ratio of isobaric to isochoric specific heats, λ is the radian wavelength, x is the position of the stack in the resonator, and β is the thermal expansion coefficient for the working gas. The thermoacoustic prime mover has a relatively low efficiency because of its natural irreversibility; heat flow between the sound field and the stack elements provides the necessary phase shift to produce sound power. It is important to note that as the operating frequency ω is raised, the critical temperature gradient ∇T_{crit} also increases.

A significant characteristic of the acoustic heat engine is its power density which can be large, especially when the operating frequency is high. An estimate can be made for the power per unit volume. For the heat flow contribution, it is given by [7]:

$$\text{Power / volume} \approx \frac{\omega}{4\pi} (T_m \beta) \frac{P_1^2}{\rho_m a^2} (\Gamma - 1) \quad (5)$$

where a is the speed of sound in the gas, ρ_m its density, and P_1 the maximum pressure amplitude of the sound. For a device operating at 20kHz, a power density due to heat flow and work flow of $\sim 0.025 \text{ W/cm}^3$ can be achieved with air at one atmosphere at a sound intensity of 143 dB. It is important to note that the power density scales directly with frequency since the system is resonant and with gas pressure. Such high power density compares very favorably with other types of heat engines and energy converters, for example thermoelectric [10] or magnetic [11].

For energy conversion from sound to electricity, a piezoelectric device was chosen over an electromagnetic device because it is compact and it can achieve high efficiency. A practical configuration is as a unimorph unit where displacements due to the sound are mechanically amplified causing a bending action of the piezo, thus generating electricity.

This introduction has presented the important elements of thermoacoustic devices that need to be scaled for device miniaturization for energy conversion.

2. Miniaturization of a Thermoacoustic Prime Mover

To reduce the acoustic device size, a scaling approach needs to be followed, if possible and the physics of how this device works has to be preserved. Going from an operating frequency of $\sim 100 \text{ Hz}$ or even 2 kHz up to 20 kHz , is quite a large step in device size reduction. In order to achieve this goal, the approach taken here is to first develop a device at $\sim 10 \text{ kHz}$, and then extend the technology for the ultrasonic range. The resonator in this work is a $\frac{1}{4}$ wavelength cylinder open at one end. Inside it are the heat exchangers and the stack. Heat is injected into this device either by means of a wire heater wound near the hot heat exchanger or directly by means of a flame or simply by thermal contact to the body generating heat. Fig. 1 shows a

schematic of an energy converter to illustrate the approach which needs to be taken in developing and scaling down the size of this device. [9] Heat excites a standing wave in a $\frac{1}{4}$ wavelength resonator and this sound wave is converted directly to electrical energy by means of a piezoelectric device.

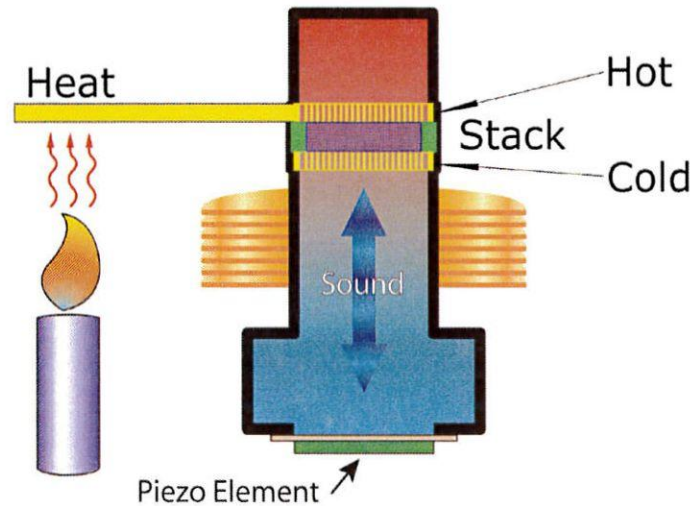


Fig.1 Basic Energy Converter

In scaling down the devices, there are important geometrical factors that need to be maintained or adjusted. The role of the thermal penetration depth δ_κ is one such factor important in scaling the stack density. It determines the spacing between stack elements for maximum acoustic power output. Ideally this spacing should be 2-3 δ_κ . Closer spacing will cause significant reduction of the device quality factor Q . Another important dimension that needs to be considered is the resonator diameter; a large cross-sectional area of the resonator provides high level of sound power. However, too large an area relative to the length of the resonator will cause a reduction in the resonator standing wave ratio, thus reducing the positive feedback; in that case the threshold ΔT for onset is increased. The scaling with size reduction of some important dimensions and their effect on physical properties are presented in Table 1.[12] The Reynolds number is a parameter which compares inertial forces to viscous forces in the fluid. It is highly reduced as the device is made smaller.

Characteristic Device Dimension "L"
Acoustic Frequency $\propto 1/L$
Thermal Time Constant $\propto L^2$
Mechanical Power Density $\propto 1/L$
Electrostatic Power Density $\propto 1/L$
Reynolds Number $\propto L^2$
Heat Flow $\propto 1/L$

Table 1. Effects of Device Size Reduction

One important feature in this table is that the thermal time constant will be greatly reduced by scaling up the operating frequency. Also, in that case heat flux, for a fixed temperature difference, will be raised.

3. Sub-Ultrasonic Heat Engine

The development of the ultrasonic devices followed a series of progressions where devices were made smaller in increments of frequency increasing up to the 20 kHz range. Fig.3 shows one such device operating at 8.8 kHz. The waveform at 8.8 kHz is that of the heat generated sound. The device is 8.6 mm long and the i.d. is 2 mm.

Onset for oscillation was at a temperature difference $\Delta T=106^{\circ}\text{C}$ at a heat flux of 0.30 watt applied to the hot side of the engine. The acoustic response curve shows the exponential build up of oscillations, characteristic of the gain of the device, followed by leveling off in the acoustic output, where the total losses are balanced by the heat flux input.

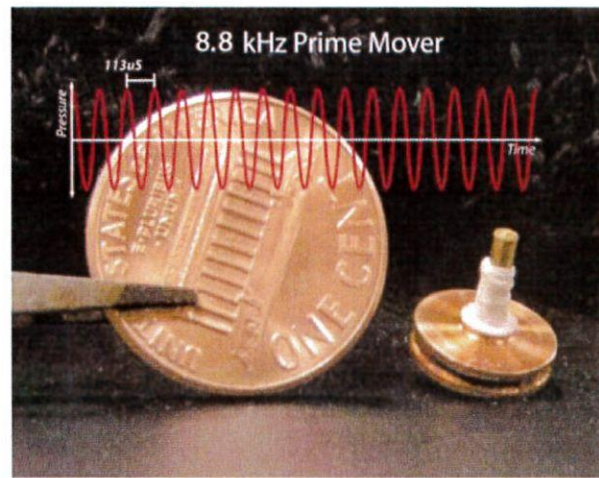


Fig. 2 Prime Mover at 8.8 kHz. This was part of a series of learning steps leading to the ultrasonic device.

4. Ultrasonic Heat Engines

For a device operating at ~ 20 kHz, the resonator length was reduced to ~ 3.4 mm long, with a bore of 1 mm, for $\frac{1}{4}$ wavelength resonator. As before, the resonator is divided in 2 sections, the hot part with its hot heat exchanger, and the cold part with its cold heat exchanger. The stack, made of random low thermal conductivity high-surface area material, is sandwiched between the two heat exchangers. It consists of stainless steel mesh made out of $10.1 \mu\text{m}$ radius wires. The working gas volume inside the resonator is 0.0027 cm^3 . A piezoelectric device (a unimorph) converts the acoustic power to electricity; it is coupled to a cavity which is attached to the open end of the resonator. The spacing between the stack filaments is $\sim 2\delta_k$, where δ_k is the thermal penetration depth. At 20 kHz this penetration depth is quite small, being $18\mu\text{m}$. The heat exchangers are made with copper screen. Fig.3 shows one of the copper heat exchangers thermally anchored to the resonator.

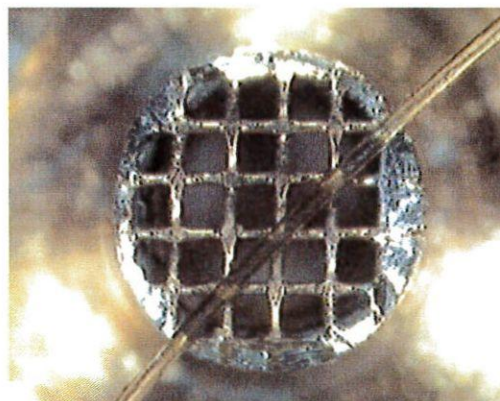


Fig. 3 Copper Heat Exchanger

A strand of hair is placed across it to show the scale of the device parts. The critical temperature gradient ∇T_{crit} is expected to be ~ 1300 K/cm. Heat is supplied to the hot side by means of a fine wire heater wrapped around the hot part of the resonator. Temperatures at the hot and cold sides of the heat exchangers are monitored by means of copper-constantan thermocouples of diameter 0.025 mm. Sound intensity is detected by the piezoelectric unimorph which was calibrated; it was not operated at its self-resonance.

Fig.4 shows the onset for oscillations and the sustained oscillations for an ultrasonic device. The threshold for oscillations occurs at ~ 1 second on this graph. Heat input is switched off at 7.5 seconds. Acoustic oscillations are at 21 kHz. The curve in Fig. 5, below the oscillation pattern, shows how the temperature difference along the stack evolves with the corresponding time. As the temperature difference increases the acoustic intensity grows. Individual oscillation cycles are not visible in fig. 4 because of the long time scale on the oscilloscope.

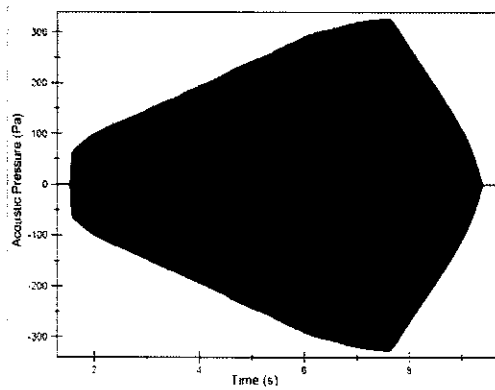


Fig. 4 Ultrasonic Oscillation Growth Pattern Detected by Piezoelectric Device.

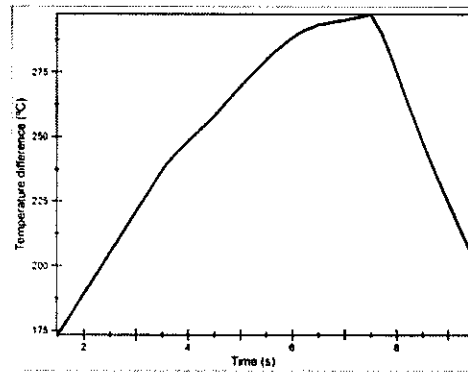


Fig. 5 Corresponding temperature difference across the engine during the run of Fig. 4.

Temperature differences ΔT at onset for oscillations varied in the range of $\Delta T = 180^\circ\text{C}$ to 200°C depending on the unit. The main difference between the various units tested (eight engines were tested), a technical issue, was the alignment of the two halves of the resonator as well as of the heat exchangers relative to each other. This explains the large variations in ΔT for onset. Calculating an experimental critical

temperature gradient for only the stack thickness would give too large a value as the temperature gradient between the hot heat exchanger and the resonator walls also plays a major role here. The generated sound was sinusoidal with no measurable harmonic content. Sound intensity levels at the piezo were 143-150 dB for a ΔT of 300°C between the heat exchangers. As the ΔT is raised the generated acoustic intensity increases (Fig. 4).

5. Discussion and Applications

Because of its potential for applications, the thermoacoustic prime mover has been studied by many groups. This has been done for relatively large devices operating normally in the few hundred Hertz frequency range [13,14]. The work presented here has extended the operating frequency range to the ultrasonic range, thus opening the field for thermoacoustic microdevices. Successful operation at such high frequencies is an achievement which is based on the fact that the development of the ultrasonic device followed very carefully the conditions necessary for initiating and sustaining oscillations in this self-sustained oscillator.

They are:

- (i) Timing in an engine is provided by heat flow between the stack and the sound field. This condition is expressed as $\omega\tau \approx 1$ where τ is the thermal relaxation time for heat exchange between stack elements and the working fluid. It is defined by $\tau = r_0^2 / 2\kappa$ where r_0 is the average distance between elements of the stack and κ is the thermal diffusivity of the fluid.
- (ii) The resonator quality factor Q is critical for initiating and sustaining the oscillations. The quality factor is defined as $Q = \omega m / r$ where m is the mass of the working fluid inside the resonator and r represents the losses (thermal, viscous, and radiative). Considering only viscous losses, the Q is $\left(\frac{3}{2} \omega \rho / \eta \right)^{1/2} R_0$ where R_0 is the radius of the resonator, η is the air viscosity and ρ is the air density.

The above conditions for generating oscillations reflect the criterion postulated by Lord Rayleigh and they are applicable to the ultrasonic range covered here [15]. Acoustic oscillations are promoted when heat is added at a condensation of the gas, and when it is extracted at the rarefaction (phase of oscillation). The thermoacoustic instability is created by an unsteady heat release which fluctuates in phase with pressure oscillations [16,17].

The onset to oscillations is a phase transition from disorder to order in a system that is far from equilibrium. In certain aspects it has similarities with a laser. Interesting features of the device developed here are:

- Fast response because of its small thermal mass (0.006J/°C); air at one atmosphere is the working fluid.
- Engine with essentially no moving parts (except for the moving air and flexing piezoelectric device).
- Environmentally friendly.
- High power density, of order 0.025W/cm³ and higher depending on operating conditions.
- Can be used as basic unit or form an array in order to achieve high power levels. Synchronization of such units will maximize power output.[18]
- Can handle a wide range of ΔT ; for the units studied here ΔT goes from 175°C to quite large values (a few hundred degrees) limited by parts in the device.
- Preliminary tests show an efficiency of ~10% of Carnot in units studied here. Higher values are expected as device alignment in fabrication improves. The overall converter efficiency is the product of the heat to acoustic part and the piezo part. This was not determined here because the piezoelectric device was not operated on resonance; it acted only as a broadband acoustic detector.
- Because the devices are small they can easily be pressurized to high levels without severe limitations due to the strength of materials.

The applications for the acoustic energy converter are extensive, ranging from solar energy harvesting to thermal management of power plants and high power electronics to space exploration.



An interesting question arises as to how high in frequency can thermoacoustic devices work. For the higher ultrasonic range the devices will have to be fabricated using MEMs technology. They are expected to perform well as long as Lord Rayleigh's criterion is met. It would seem that heat transfer process is slow and hence it would limit thermoacoustic processes at high frequencies. The results presented here show that it is not the case, since the device mass is small, the distances are short, and heat transfer is increased [19].

As the devices are reduced in size, mean free path effects in the working gas will start to play an important role in some of the processes, like thermal conductivity and viscous dissipation involved in this type of energy converter. An important parameter that determines the heat transfer and flow regimes is the Knudsen number Kn which is the mean free path of the gas particles divided by characteristic dimensions such as the penetration depth. For Kn less than 0.01, the system is in the continuum regime with no-slip at interface of stack element and working gas. At 20 kHz operating frequency in devices presented here, $Kn = 0.0125$ and the continuum conditions on transport still apply. However, operating at higher frequencies will require slip-flow boundary conditions as the slip-flow regime is approached. The flow may then be modeled by the Navier-Stokes equations with a slip boundary condition.

The ultrasonic energy converter presented here opens the thermoacoustic field to a new range of operating frequencies and acoustic microdevices. Its high power density, especially when pressurized, and simple device geometry make it attractive for a wide range of applications, particularly when in array configuration.

Acknowledgements

This work was supported by the US Army Space & Missile Defense Command and the University of Utah.

References

1. S. Backhaus, E. Tward, and M. Pelach, "Traveling wave thermoacoustic electric generator", *Appl. Phys. Lett.* **85**, 1085 (2004).
2. J.J. Wollan and G. Swift, "Development of a Thermoacoustic Natural Gas Liquefier – Update", American Gas Association Operations Conference, Houston, April, 29, 2001.
3. L. Zoontjens et al, "Feasibility Study of an Automotive Thermoacoustic Refrigerator", *Proc. of Acoustics 2005*, Busseton, Australia, p. 373-379, (2005).
4. F. Zink, J.S. Viperman, and L.A. Schaefer, "Environmental motivation to switch to thermoacoustic refrigeration", *Applied Thermal Engineering* **30**, 119 (2010).
5. Rott, N. "Thermoacoustics". *Adv. Appl. Mech.* **20**, 135 (1980).
6. J.C. Wheatley et al, "Understanding some simple phenomena in thermoacoustics" *Am. J. Phys.* **53**, 147 (1985).
7. G.W. Swift, "Thermoacoustic Engines" *J. Acoust. Soc. Am.* **84**, 1145 (1988).
8. A.B. Pippard, "The Physics of Vibration", Cambridge University Press, 1989, pg.41 and 359.
9. O.G. Symko et al, "Design and development of high frequency thermoacoustic engines for thermal management in microelectronics", *Microelectronics Journal* **35**, 185 (2004).
10. D.T. Crane et al, "Performance Results of a High-Power Density Thermoelectric Generator", *J. of Electronic Materials* **38**, 1375 (2009)
11. V. Srivastava et al, "The direct conversion of heat to electricity using multiferroic alloys", *Adv. Energy Mater.* **1**, 97 (2011).
12. R. Drexler, "Nanosystems", J. Wiley and Sons, Inc. 1992, p. 24.
13. K.T. Feldman and R.L. Carter, "A study of heat driven pressure oscillations in gas", *Journal of Heat Transfer*, Vol. **92**, 1970, p.536.
14. A.A. Atchley, "Analysis of the initial buildup of oscillations in thermoacoustic prime mover", *J. Acoust. Soc. Am.* **95**, 1661 (1994).



15. J.S. Rayleigh, "Theory of Sound" Dover Publications, Vol. II, pg.226, 1945.
16. K.I Matveev and F.E.C. Culick, "A study of the transition to instability in a Rijke Tube with axial temperature gradient", J. of Sound and Vibration, 264, 689 (2003).
17. G. Huelsz and E. Ramos, "On the phase difference of the temperature and pressure waves in the thermoacoustic effect", Intern. Commun. in Heat and Mass Transfer, 22, 71 (1995).
18. A.B. Pippard "The Physics of Vibration", Cambridge University Press, 1989, pg. 365.
19. P. Tabeling "Introduction to Microfluidics", Oxford University Press, (2005).



Tables

Characteristic Device Dimension “L”

Acoustic Frequency $\propto 1/L$

Thermal Time Constant $\propto L^2$

Mechanical Power Density $\propto 1/L$

Electrostatic Power Density $\propto 1/L$

Reynolds Number $\propto L^2$

Heat Flow $\propto 1/L$

Table 1. Effects of Device Size Reduction



Figure Captions:

- Fig. 1 Basic Energy Converter
- Fig. 2 Prime Mover at 8.8 kHz
- Fig. 3 Copper Heat Exchanger
- Fig. 4 Ultrasonic Oscillation Growth Pattern Detected by Piezoelectric Device
- Fig. 5 Corresponding temperature difference across the engine driving the run of Fig. 4

Figures

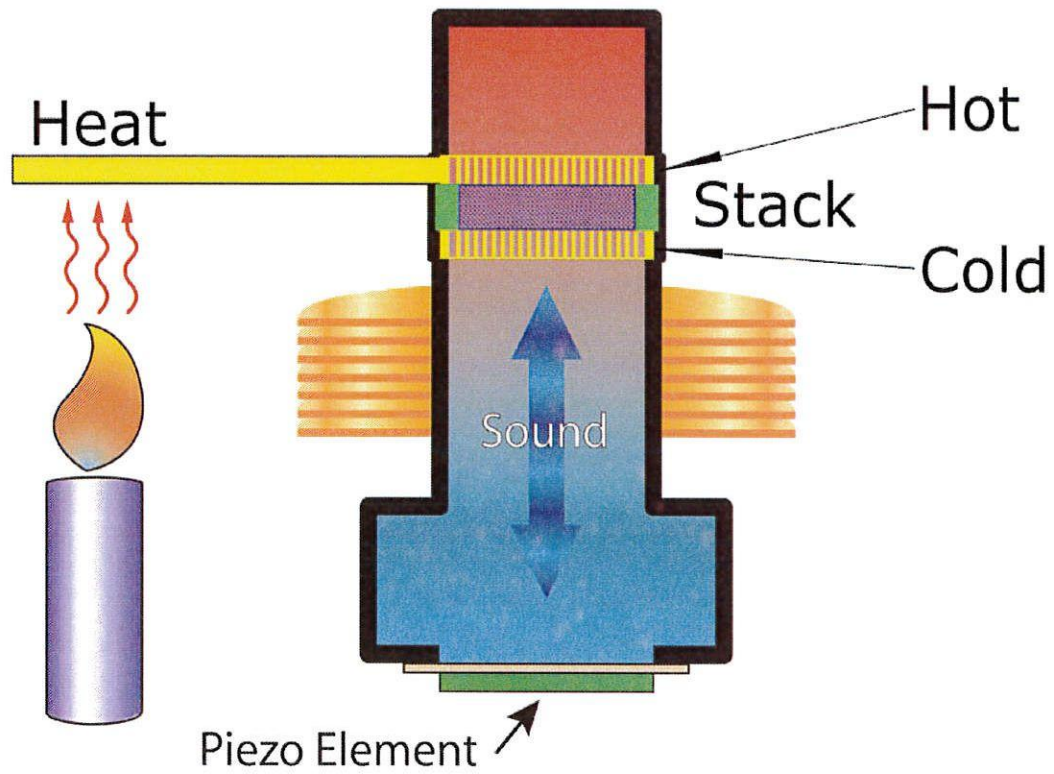


Figure 1: Basic Energy Converter

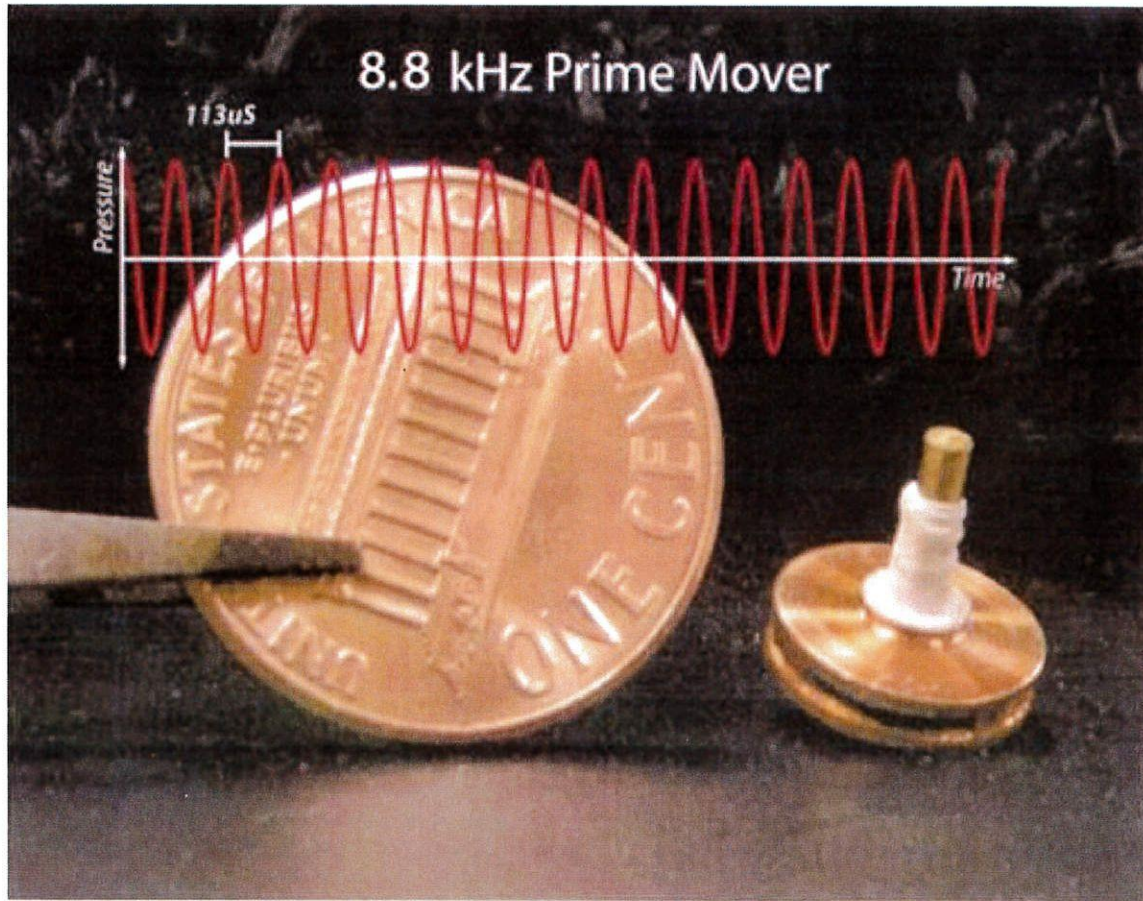


Figure 2: Prime Mover at 8.8 kHz. This was a series of learning steps leading to the ultrasonic device.

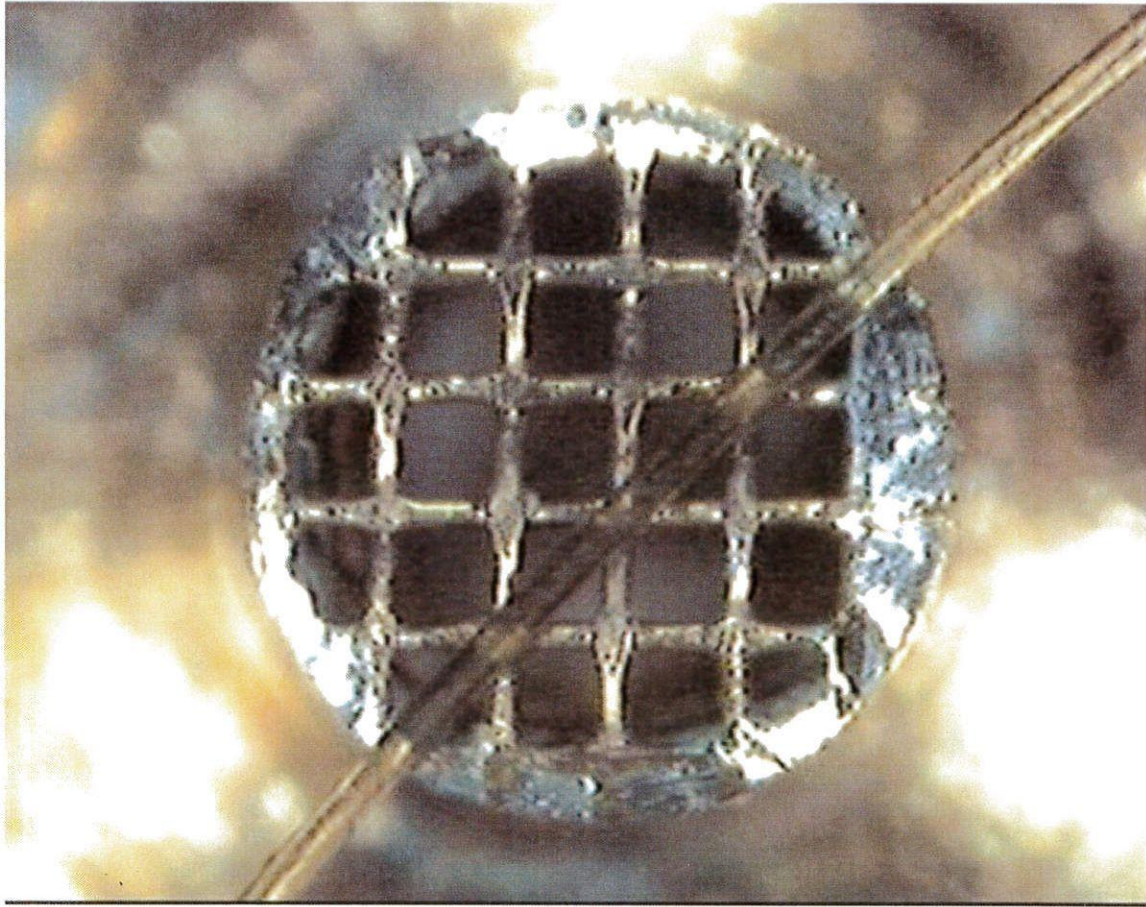


Figure 3: Copper Heat Exchanger.

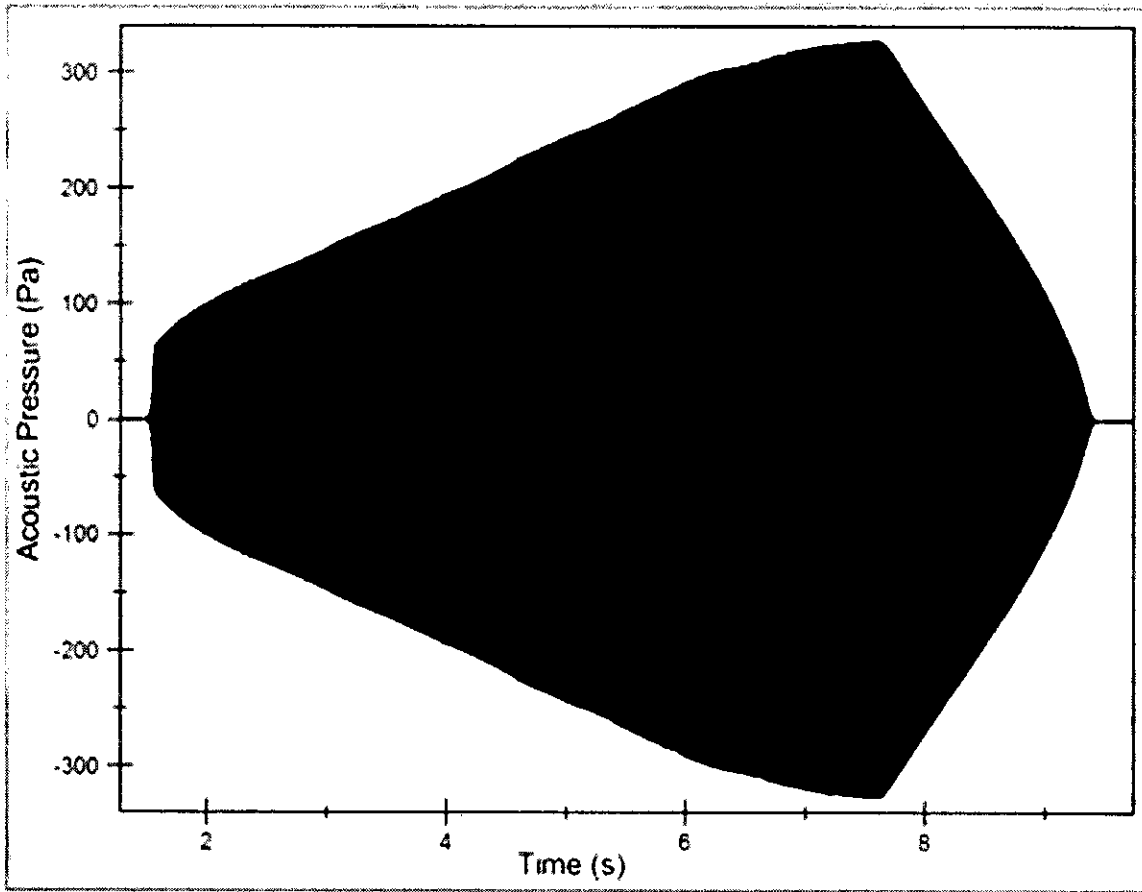


Figure 4: Ultrasonic Oscillation Growth Pattern Detected by Piezoelectric Device.

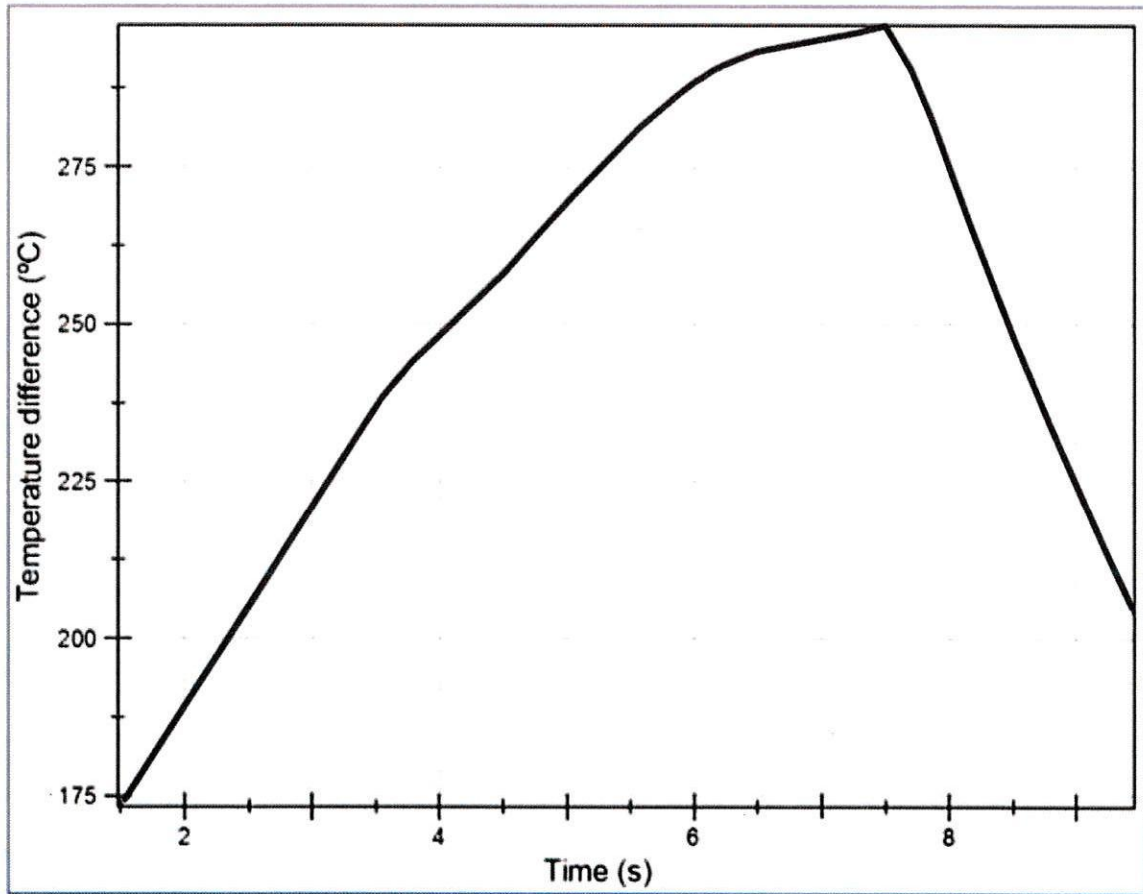


Figure 5: Corresponding temperature difference across the engine during the run of Fig. 4.